Mechanical behavior of nanocrystalline Cu and Pd

G.W. Nieman and J.R. Weertman
Department of Materials Science and Engineering, Northwestern University, Evanston, Illinois 60208

R.W. Siegel
Materials Science Division, Argonne National Laboratory, Argonne, Illinois 60439

(Received 30 July 1990; accepted 23 January 1991)

This report gives results of a study of the bulk mechanical properties of samples of nanocrystalline Cu and Pd consolidated from powders prepared by inert gas condensation. Fourier analysis x-ray diffraction techniques, used to determine average grain size and mean lattice strains of the as-consolidated samples, show grain sizes in the range of 3–50 nm and lattice strains ranging from 0.02–3%. Sample densities range from 97–72% of the density of a coarse-grained standard. Microhardness of the nanocrystalline samples exceeds that of annealed, coarse-grained samples by a factor of 2–5, despite indications that sample porosity reduces hardness values below the ultimate value. Uniaxial tensile strength of the nanocrystalline samples is similarly elevated above the value of the coarse-grained standard samples. Restrictions on dislocation generation and mobility imposed by ultrafine grain size are believed to be the dominant factor in raising strength. Residual stress may also play a role. Room temperature diffusional creep, predicted to be appreciable in nanocrystalline samples, was not found. Instead, samples appear to show logarithmic creep that is much smaller than the predicted Coble creep.

I. INTRODUCTION

Grain size is known to have a profound effect on the mechanical behavior of materials, in particular, on the yield stress and the diffusional creep rate. This effect has been well-studied for grain sizes down to about 1 μm. Study of mechanical effects for materials with smaller grain size has been limited by the difficulty of producing bulk materials with such grain sizes. The inert gas condensation process followed by *in situ* consolidation has recently been used[1–7] to produce ultrafine-grained metals and ceramics with a narrow grain size distribution. By adjusting the synthesis conditions, the average grain size can be made to fall in the 5–50 nm size range. The present paper describes the results of a study of the mechanical behavior of bulk specimens of Cu and Pd made by cold compaction of nanocrystalline particles produced by this method. Uniaxial tensile stress-strain tests and constant load creep tests were performed at room temperature on bulk materials with grain sizes in the range of 5–50 nm; additional information was furnished by Vickers microhardness measurements. The results are related to material properties that include grain size and density, and to processing variables such as heat treatment and sample preparation. Related short reports have been given in Refs. 8 and 9.

The dependence of tensile yield stress on grain size in metals and ceramics is well established for micrometer and larger grain sizes. Yield stress σ_y, for materials with grain size d, is found to follow the Hall–Petch relation[10,11]:

$$\sigma_y = \sigma_0 + kd^{-1/2} \quad (1)$$

where σ_0 is the friction stress and k is a constant commonly interpreted to represent the stress needed to extend dislocation activity into grains adjacent to grains that have already yielded. Flow stress at a particular strain follows a relation similar to Eq. (1).[12–14]

In the case of deformation by diffusional creep at low homologous temperatures (T/T_m), grain boundary diffusion will predominate over bulk diffusion effects. Coble[15] has shown that under these conditions the diffusion creep rate $\dot{\epsilon}$ is given by:

$$\dot{\epsilon} = \frac{B\sigma\Omega\delta D_b}{d^3kT} \quad (2)$$

where B is a constant, σ is the applied stress, Ω is the atomic volume, δ is the grain boundary thickness, and D_b is the grain boundary diffusion coefficient. According to Eqs. (1) and (2), reduction of grain size from conventional values to nanometer size should lead to drastic changes in mechanical properties. Equation (1) predicts a strengthening as d decreases, but the inverse cube dependence of $\dot{\epsilon}$ on d in Eq. (2) indicates diffusional creep could become important at nanometer grain sizes even at room temperature. Disagreement exists about the effects on mechanical properties of grain

https://doi.org/10.1557/JMR.1991.1012 Published online by Cambridge University Press

sizes less than 1 μm,[12,16] and for nanometer grain sizes there is disagreement over the properties of the grain boundaries. Several studies have been interpreted to show that nanocrystalline grain boundaries have a novel structure.[1–3,17–20] A study of self-diffusion in nanocrystalline copper indicated a diffusivity that is 10^3 faster than grain boundary diffusion in coarse-grained Cu.[21] The possibility of greatly enhanced Coble creep was used to explain observations on the formability of ceramics[22,23] and on the grain size dependence of microhardness in nanocrystalline Cu and Pd.[24] Other investigations have concluded, however, that nanocrystalline grain boundaries are not so different from ordinary grain boundaries.[25–29]

Nanocrystalline grain size imposes dimensional constraints on deformation mechanisms such as dislocation generation and interactions or twin formation. As grain diameter decreases to the length of a few Burgers vectors and grain volume decreases dramatically with respect to grain boundary volume, deformation mechanisms must reflect size effects. Bulk mechanical behavior may differ from that of conventional grain size materials. The goal of the present work is to characterize the room temperature mechanical behavior of bulk nanocrystalline samples of two pure fcc metals, Cu and Pd, with grain sizes in the 5–50 nm range. Of particular interest are the effects of grain size on yield and flow stress, microhardness, and diffusional creep. To this end, stress-strain, microhardness, and creep experiments were carried out on bulk specimens of nanocrystalline Cu and Pd. The results are compared to behavior of annealed, coarse-grained samples tested under similar conditions.

II. PROCESSING AND DENSITY MEASUREMENTS OF NANOCRYSTALLINE SAMPLES

A. Material processing

The nanocrystalline samples used for this study were produced by inert gas condensation. Details of sample synthesis and processing have been described elsewhere.[5–7] Samples were synthesized from high purity precursor metals (Cu or Pd) evaporated near the melting temperature into approximately 650 Pa of He gas in the chamber. After an evaporation/gas-condensation run, the vacuum was returned to near the level obtained after baking the chamber walls and prior to evaporation, $\approx 1 \times 10^{-5}$ Pa. Subsequently the collected gas-condensed powder was consolidated in a compaction unit that was sealed at this vacuum pressure and removed from active pumping. Consolidation was accomplished at room temperature using a pressure of 1.4 GPa, reached within 90 s. The pressure was held at this value for 3 min, then released over a period of approximately 2 min.

Typical dimensions of the disk-shaped samples produced by this consolidation are 8 to 9 mm in diameter and 0.15 to 0.45 mm thickness. As-consolidated samples were studied by optical and scanning electron microscopy to identify defects that might influence mechanical behavior. Major features identified include heterogeneous texture in low compacted rims, radial rim cracks, polygonalized and irregular surface cracks, string-like and angular features, low-relief surface topography, and small cavities. Polishing removed most surface features, including cracks; but string-like agglomerates remained in some polished samples. A significant low-compacted rim occurred in highly compacted pellets <0.25 mm thick. In thicker samples this rim is reduced in width and may not exist. Rim material was not used in the mechanical test specimens.

B. Density measurements

Precision density measurements, based on the Archimedes principle, were made on several Pd and Cu samples by weighing them in ethyl phthalate and air. All measurements were made using a Mettler precision analytical balance having a nominal sensitivity of 10 μg, although the last significant figure is of low precision. Each sample was first weighed in air. It was then prepared for weighing in liquid by submersing the sample in ethyl phthalate in an ultrasonic bath for a minimum of 10 min to remove any air trapped on the surface of the sample or in pores. The samples were then weighed in ethyl phthalate. Density ρ as a fraction of the standard density ρ_{std}, taken from the CRC handbook,[30] was determined by the equation:

$$\frac{\rho}{\rho_{std}} = \frac{MW_A \times (MW_{A-std} - MW_{L-std})}{MW_{A-std} \times (MW_A - MW_L)} \quad (3)$$

where MW_A = measured weight of sample in air − air tare
MW_{A-std} = measured weight of standard in air − air tare
MW_L = measured weight of sample in liquid − liquid tare
MW_{L-std} = measured weight of standard in liquid − liquid tare

Density measurement results for Pd and Cu samples made by this method are given in Table I. The density of seven nanocrystalline Pd samples ranges from a maximum of about 96% to a minimum of 83% of the fully dense value. The mean is 86% of the standard density, with a standard deviation of ±3.2%. Representative density data for 27 measurements on 10 Cu samples range from a maximum of about 97% to a minimum of 72%, with a mean of 90.5% and a standard deviation of ±6.3%. The standard deviation for 40 measurements of a coarse-grained Cu standard sample, made at the time the nanocrystalline samples were

https://doi.org/10.1557/JMR.1991.1012 Published online by Cambridge University Press

TABLE I. Precision density data for some nanocrystalline Pd and Cu samples.

Sample	Density (10^3 kg/m^3)	% of standard
Pd8031	11.580	96.34
Pd8052	10.186	84.74
Pd8052	9.956	82.83
Pd8101	10.519	87.51
Pd1202	11.038	91.83
Pd1203	10.394	86.48
Pd1205	10.081	83.87
Cu2232	6.402	71.66
Cu2271	8.030	89.88
Cu3012	8.563	95.85
Cu3021	7.807	87.38
Cu3061	8.623	96.52
Cu3071	8.343	93.39
Cu3081	8.688	97.25
Cu3091	8.495	95.09

tested, is 0.2%, indicating a measurement precision of this magnitude. Results for several nanocrystalline Cu samples retested at another time agree to within 1 to 5%. Density measurements were not made on the two Cu samples for which tensile and creep test data are reported here.

C. Discussion of density results

Consolidation of metal particles has been carefully studied because of interest in powder metal fabrication.[31–33] With cold compaction, 98.5% of the fully dense value has been achieved using a compaction stress equal to 3 $\sigma_{y,cw}$, the cold-worked yield stress. Assuming $\sigma_{y,cw}$ is proportional to $d^{-1/2}$ for nanocrystalline particle size, very large compaction stresses are predicted to be needed to cause yielding and achieve high densities. The maximum compressive stress used in the present study (1.4 GPa) is, however, somewhat less than the minimum stress σ_m required to activate a Frank–Read source in 10 nm grain size palladium or copper, if the source length is limited to the grain size ($\sigma_m \approx 2Gb/d$, where G is the shear modulus, b is the magnitude of the Burgers vector, and d the grain size). Consequently, particles of this size may not deform greatly during compaction, and the consolidated sample may be relatively porous and brittle. Cold compaction may also result in formation of delamination microcracks in the plane normal to the compaction stress, especially for elastically strong materials.

The 97% maximum density achieved in the present work is close to the maximum value for cold-compaction at high pressures determined by Gutmanas.[33] In general, the densities shown in Table I are lower limits, since these measurements include the very porous low-compacted rims. The large variation in density, from 96% to 83% of the standard Pd value, for example, results from a number of factors. Probably the most significant is the variability from sample to sample in the size of the low-compacted rim and the variability of the compaction efficiency in this area. Optical and SEM observations show that these rims are highly porous and that they contain a large number of cracks. A second factor is surface porosity in the high-compacted part of the pellet. Some surface pores are likely to be connected to pores below the surface, and this volume may or may not be accessible to the ethyl phthalate.

III. DETERMINATION OF GRAIN SIZE

Investigation of the effect of grain size on the mechanical properties of nanocrystalline palladium and copper requires accurate knowledge of the grain size and size distribution for the test specimens. Both x-ray diffraction (XRD) analysis of line broadening[34–37] and transmission electron microscopy (TEM) measurements have been used in recent studies to determine grain size and grain size distributions.[4,5,7,29] In general, somewhat different estimates of mean size may result due to weighting factor differences of the method employed and to systematic and random errors. For example, TEM is especially useful for observing twinning and for making estimates of grain size distributions, but the results are based on a small number of grains and the process is destructive to the sample. Several XRD methods are used. Fourier analysis XRD methods give an area-weighted estimate of mean grain size, while the commonly used Scherrer XRD method[34,36] gives a volume-weighted grain size estimate. Both XRD estimates are based on a large number of grains and can be used for consolidated or unconsolidated samples with little sample preparation.

Previous studies by TEM of nanocrystalline samples produced by inert gas condensation indicate that the method produces narrow grain size distributions.[4,5] In principle, the second derivative of the XRD Fourier coefficients with respect to scattering length gives the grain size distribution. However, the analytical precision of such estimates based on the raw XRD data is not good. A qualitative estimate of the width of a distribution can also be made by comparison of the mean grain size determined by the area-averaged Fourier method with the volume-averaged Scherrer method estimate. Close agreement between these results indicates a narrow size distribution.

It may be difficult by XRD methods to distinguish grains separated by ordinary boundaries from twins and grain subdomains, such as dislocation cells. Significant cell development does not occur in these ultrafine grains,[27,38] but twins and stacking faults have been observed.[38] Broadening caused by the presence of twins and stacking faults results both in differences in broadening of the 111 and 200 lines and in unusual peak

https://doi.org/10.1557/JMR.1991.1012 Published online by Cambridge University Press

shifts between them,[35] which can be used to differentiate among grain size, twinning, and faulting effects.

The present study of consolidated nanocrystalline samples employs Fourier analysis XRD methods, including those of Warren–Averbach and Nandi *et al.*[34–37] Fourier analysis gives an estimate of the mean grain size from the mean coherent scattering length normal to the diffraction direction. An estimate of mean strain in this direction is also obtained. Factors other than fine grain size and strain that contribute to line broadening, such as the instrument slit function, can be distinguished.[34–36] At least two orders of a given reflection are needed to estimate grain size and strains by Warren–Averbach (WA) analysis. An extension of this method by Nandi *et al.*[37] allows Fourier analysis to be applied to a single order of a peak, under relatively unrestricted conditions. In general, single peak analysis underestimates the grain size, particularly for samples with narrow size distributions. The full-width-half-maximum for the Scherrer method for grain size estimates, and reconstructions of the low 2θ tail of some 222 diffraction peaks, were calculated by a least-squares fit of the diffraction profile to a pseudo-Voigt function.[39] A more detailed description of the XRD analysis used here for the nanocrystalline samples is given in Ref. 40.

Mean grain size and lattice strain data for 17 as-consolidated nanocrystalline palladium and copper samples are shown in Table II. Note that the grain size and strain values given are estimates of average values, based on the coherent scattering length normal to the indicated diffraction plane. The double peak grain size estimates are based on the 111 and 222 peaks, except where indicated. The mean strains in Table II were determined by the double peak analysis unless no grain size value for this estimate is given, in which case strain was estimated from the 111 peak only. Diffraction data for one of the smallest grain size samples are shown in Fig. 1. Table II shows that estimates of average grain size calculated from Fourier analysis techniques for the Pd samples range from about 3 to 21 nm, while estimates for copper samples range from about 4 to 50 nm.

TABLE II. Comparison of particle size estimates (nm) obtained by several methods, and mean long-range strains ($\langle\epsilon_{10}^2\rangle^{1/2}$) calculated at 10 Å scattering length from double peak XRD data.

Sample	Scherrer	Single-peak		Double-peak	$\langle\epsilon_{10}^2\rangle^{1/2}$ ($\times 10^{-3}$)
		111 peak	200 peak		
Pd7061[a]	54	11		11	1.4
Pd8011[b]	14		11	15	13.0
Pd8031	24		14		0.7
Pd8051[a]	7	3		3	2.2
Pd8052[a]	8	4		4	0.8
Pd8101[b]	30	5	6	21	34.0
Pd1202[a]	37	17		15	1.7
Pd1203[a]	28	12		8	3.2
Pd1205[a]	8	5		4	3.6
Cu1103	60	50			0.2
Cu1104[a]	65	33		25	4.0
Cu2221[a]	20	6	4	6	1.8
Cu2232[a,c]	15	5	5	5	3.1
Cu2261[a]	20	6	4	6	0.6
Cu2271[a]	16	6	4	6	1.0
Cu3012[a]	30	10	7	15	12.0
Cu3091[a,d]	31	8	6	8	1.5

[a]111–222 peaks used for double peak estimate.
[b]200–400 peaks used for double peak estimate.
[c]Samples consolidated in air.
[d]Samples evaporated from a Cu_7–Si alloy.

Comparison of estimates by the two Fourier transform methods shows close agreement in all cases, with differences on the order of 10–50%. Typically, single peak grain size estimates determined for different peaks of the same sample agree within 10–25%. Good agreement between the 111 and 200 peaks suggests that the particles are equiaxed. These XRD grain size estimates and conclusions about equiaxed grain shape agree with results from TEM measurements carried out on consolidated Pd samples made under similar evaporation conditions,[27] and with preliminary TEM estimates for some of the Cu samples.

A qualitative estimate of the grain size distribution is obtained by comparison of the volume-averaged Scherrer method and the area-averaged Warren–Averbach method results, since the Scherrer method is more heavily weighted toward large particles than the Warren–Averbach technique. The reasonably good agreement between the two estimates (Table II) indicates a narrow grain size distribution for most of the samples, in agreement with previous determinations by TEM methods.

The precision for grain size estimates determined by these Fourier methods has been shown to be as good as 10–15%.[35,37] However, a practical estimate for the present study is 10–25% for the smallest grain sizes (<20 nm) to as high as 50–100% for the largest sizes (≥50 nm). This error estimate is based on observation of the magnitude of changes in the size estimate that result from small changes in the analytical procedure, such as varying the background level, as well as on the reproducibility of repeated analyses of a single sample.

For both Pd and Cu samples, mean lattice strains in the 111 direction are on the order of 5×10^{-3}, ranging from about 2×10^{-4} to 3×10^{-2}, i.e., about 0.02 to 3%. This finding is consistent with conclusions drawn from HREM observations of nanocrystalline Pd[38] and Pt,[41] and with TEM observations on a number of fine-grained metal powders by Easterling and Thölén.[42] Similar strains were determined by an XRD method in nanocrystalline Ru and RuAl produced by high energy ball milling.[43]

https://doi.org/10.1557/JMR.1991.1012 Published online by Cambridge University Press

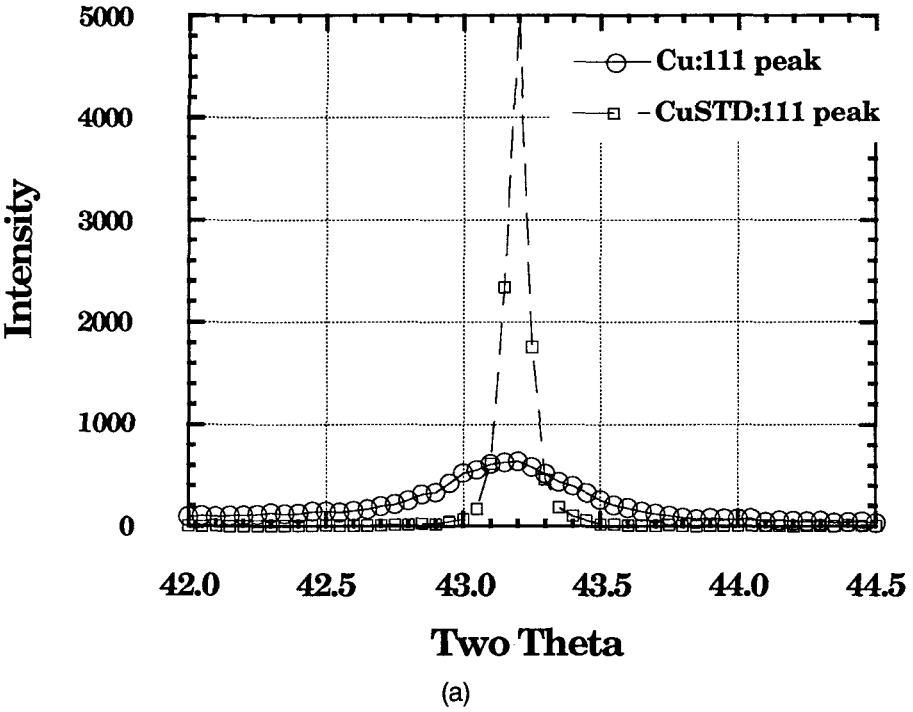

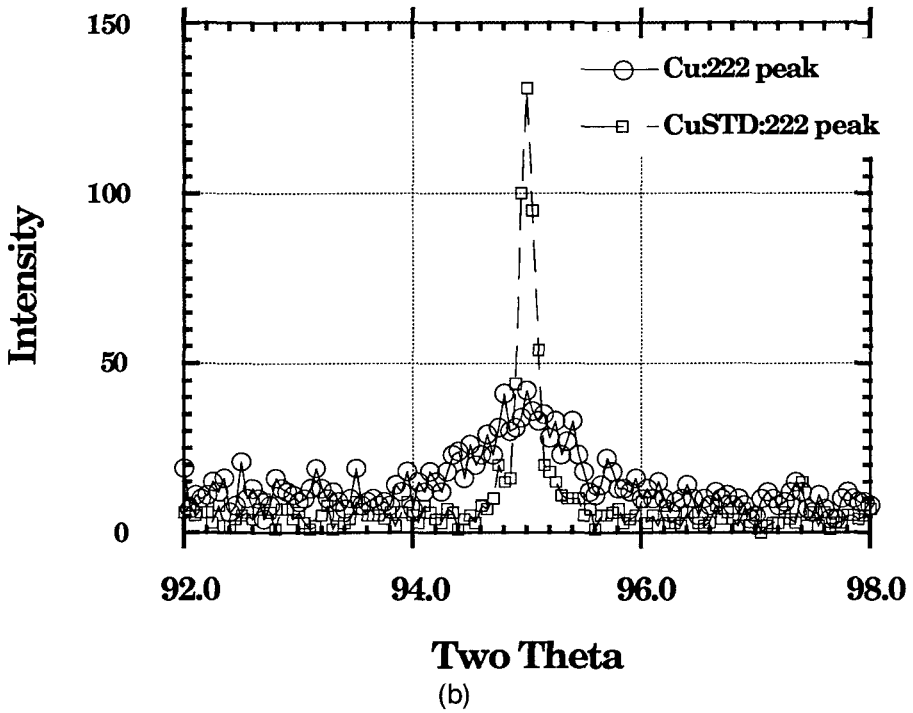

FIG. 1. X-ray diffraction profiles for the 111 (a) and 222 (b) peaks of nanocrystalline and coarse-grained Cu samples. Note the broadening of the tail regions for the nanocrystalline samples and the similar background levels of all samples.

It should be noted that in Fig. 1 there is little apparent difference in the background scattering level for the nanocrystalline and coarse-grained samples. Results of more than twenty scans of the 111, 200, 311, and 222 peaks show that the background scattering level of the nanocrystalline Cu samples is the same, given the statistical fluctuations of the background for the detector used, as for that found in four scans of the annealed, coarse-grained standard Cu sample used to determine the instrument function. This is in contrast to an earlier report on nanocrystalline Fe.[3]

The data in Table II show that very small mean grain sizes (5–10 nm) and apparently narrow size distributions can be routinely produced in pure Pd and Cu by inert gas condensation. Nonetheless, samples produced under essentially identical evaporation conditions can have quite different mean grain sizes. Size distributions have not been determined rigorously, but

https://doi.org/10.1557/JMR.1991.1012 Published online by Cambridge University Press

are suggested to be narrow. Since size distributions as well as mean sizes may influence mechanical and other properties, failure to determine distributions accurately leaves a gap in the ability to interpret experimental data used to investigate grain size dependent (mechanical) properties.

IV. MECHANICAL TESTING OF THE SAMPLES

Vickers microhardness tests, uniaxial tension tests, and constant load creep tests were performed at room temperature on the nanocrystalline Pd and Cu samples to evaluate the effects of nanocrystalline grain size on mechanical properties. Several annealed coarse-grained Pd and Cu samples were tested under conditions similar to those of the nanocrystalline samples for comparison. The typical grain size of the coarse-grained Cu used in this study is 50 μm, while the typical grain size of coarse-grained Pd is 100 μm. Grain sizes used below for the nanocrystalline samples are those obtained from the Warren–Averbach double peak XRD method (Table II).

A. Vickers microhardness measurements

Microhardness tests were carried out to investigate the as-compacted hardness of eight nanocrystalline Pd samples and seven nanocrystalline Cu samples. The effect of annealing on hardness was also examined. The microhardness measurements were made using a Buehler Micromet II microhardness tester. A load of 100 g was applied for 20 s. Varying the time of load application between 5 and 30 s did not affect the measured hardness value. The mean diagonal length of the indents was on the order of 25 μm for the nanocrystalline Pd tested, in which case 6×10^6 grains 10 nm in diameter can be intersected by the indenter. For pyramidal indenters such as the Vickers indenter, hardness is empirically related to the cold-worked yield stress[44] by the relation $H_v/\sigma_y \approx 3$. It follows that for material that exhibits Hall–Petch behavior, hardness H_v should be related to grain size d, by

$$H_v \approx H_0 + k_H d^{-1/2} \quad (4)$$

where H_0 and k_H are constants. Hardness variations are known to occur with change in load, crystallographic orientation, porosity, and depth of penetration.[45,46] Microhardness measurements give the net effect of strengthening imparted by nanocrystalline grain size and the weakening effect of processing flaws. A distribution of flaws would cause spatial variability in H_v. Surface roughness also could contribute to variation in H_v with position. Another source of spatial variability in hardness is a heterogeneous distribution of residual stresses introduced during consolidation by irregularities at the die/sample interface.

Figure 2(a) shows microhardness traverses across eight as-compacted nanocrystalline Pd samples and one coarse-grained (100 μm) sample. The grain size of the nanocrystalline samples ranges from 3 to 21 nm. There is a large spatial variability in hardness. The average hardness of the nanocrystalline samples is 3.1 ± 0.5 GPa, about four times larger than for the 100 μm standard sample (0.76 ± 0.05 GPa). Individual hardness measurements vary from a high of 4.3 GPa to a low of 2.2 GPa, both extremes found in samples with a mean grain size of 15 nm. Less spatial variability in hardness is seen in as-compacted nanocrystalline Cu [Fig. 2(b)]. The average hardness of the as-compacted nanocrystalline Cu samples in the 6 to 15 nm grain size range is 2.3 ± 0.1 GPa, about five times that of the 50 μm grain size Cu (0.45 ± 0.02 GPa). The 25 and 50 nm grain size samples are noticeably softer. Individual hardness measurements obtained for the nanocrystalline Cu samples ranged from 2.6 GPa for a sample with a grain size of 6 nm to 0.8 GPa for a sample with a grain size of 50 nm.

The effect of surface polishing on microhardness was examined. Four nanocrystalline Pd samples with grain sizes of 5–7 nm and one 100 μm grain size Pd sample were polished to 1 μm with silicon carbide paper. Two nanocrystalline Cu samples were polished to 0.25 μm using diamond paste. The samples were not annealed to reduce any surface stresses introduced by polishing. Comparison of microhardness data for Pd in Figs. 2(a) and 3 shows that polishing reduces the substantial spatial variability in H_v, but does not change the mean hardness. The standard deviation of the Pd measurements is reduced from about 15% of the mean to about 5%. Spatial variability is less pronounced in the as-compacted Cu samples tested, so there is little improvement with polishing. The observations that (a) porosity, surface roughness, and small flaws are present on the as-compacted sample surface; and (b) polishing reduces the spread in measured hardness values, but not the mean hardness, support the idea that surface flaws and localized surface stresses introduced by the compaction process are responsible for the observed microhardness variability.

Microhardness data were analyzed to investigate if grain size-dependent strengthening, analogous to Hall–Petch strengthening, is present in nanocrystalline samples. Uncertainty of 10–50% in the measured grain size, together with the spatial variability in the measured hardness values, makes it necessary to draw conclusions cautiously about the relationship between hardness and grain size in the nanocrystalline Pd. A plot of H_v vs $d^{-1/2}$ for Pd (Fig. 4) does show a large increase in hardness as grain size drops below 100 μm down into the 5 nm size range. However, a constant hardening rate (H_v vs $d^{-1/2}$) was not observed from coarse-grained

https://doi.org/10.1557/JMR.1991.1012 Published online by Cambridge University Press

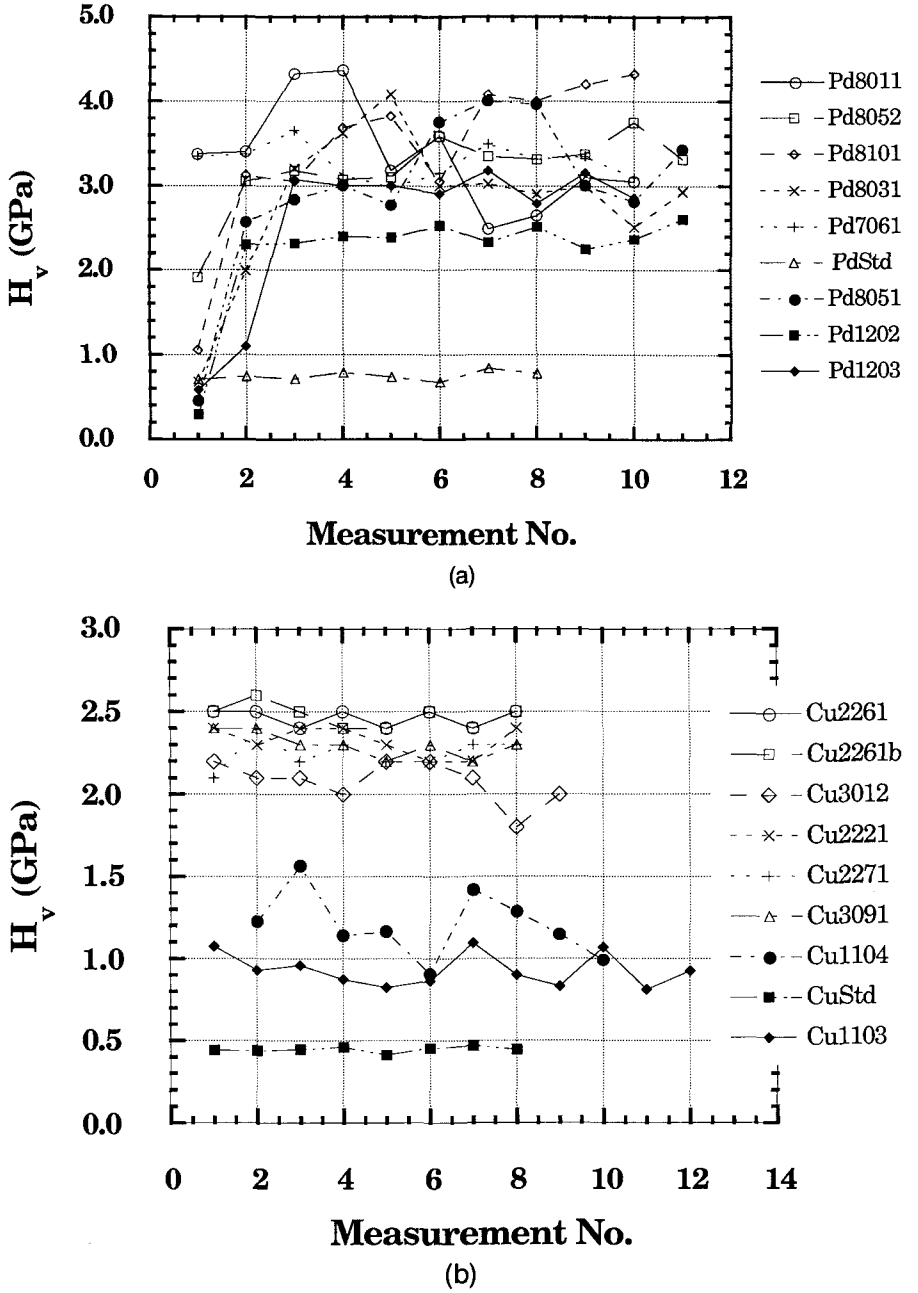

FIG. 2. Vickers microhardness of (a) as-compacted nanocrystalline and coarse-grained Pd; (b) as-compacted nanocrystalline and coarse-grained Cu. Measurement 1 for some nanocrystalline Pd samples is from low-compacted rim area. See Table II for respective grain sizes.

to nanocrystalline samples as the Hall–Petch relation predicts. Note that the relationship between H_v and $d^{-1/2}$ is about the same for the as-compacted samples as for those that have been polished. The well-polished Pd samples, including five nanocrystalline samples, show a slope of 5 MPa$\sqrt{\text{mm}}$ with an intercept of 834 MPa (Fig. 4) compared to 6 MPa$\sqrt{\text{mm}}$ and 1030 MPa for the as-compacted data. Microhardness data for as-consolidated Cu are plotted as a function of $d^{-1/2}$ in Fig. 5. Also shown in this figure are data for the 0.2% offset yield stress for two nanocrystalline Cu samples and a coarse-grained sample, and measurements by Hansen and Ralph[47] of flow stress in Cu with conventional grain sizes. The microhardness data appear to follow a linear relationship between H_v and $d^{-1/2}$, with a slope of 4.5 MPa$\sqrt{\text{mm}}$ and an intercept of 430 MPa. The yield stress data give a much smaller slope and intercept of 0.6 MPa$\sqrt{\text{mm}}$ and 80 MPa, respectively. However, the flow stress results closely parallel the microhardness results.

Yet another indication of grain size-dependent strengthening is obtained by plotting maximum rather than mean H_v vs $d^{-1/2}$. The maximum hardness may be interpreted to represent the hardness of areas that are relatively free of strength-reducing flaws, and therefore should come closest to the true hardness resulting from

https://doi.org/10.1557/JMR.1991.1012 Published online by Cambridge University Press

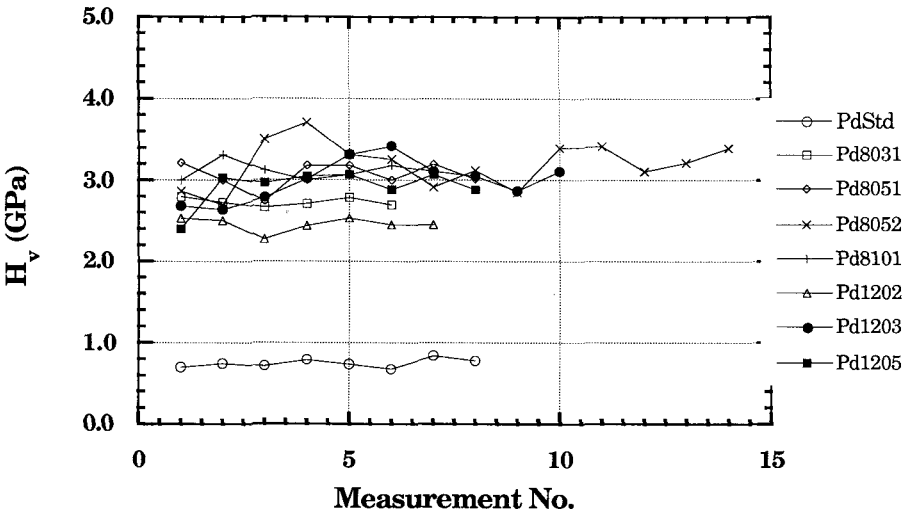

FIG. 3. Vickers microhardness of several polished nanocrystalline Pd samples compared to a polished coarse-grained (100 μm) Pd sample.

fine grain size. A plot of these data for as-consolidated Cu and Pd is presented in Fig. 6. As before, the nanocrystalline Pd samples do not show a pronounced trend in hardness. The Cu samples again show strengthening with decrease in grain size in the nanocrystalline size range, giving a slope of 4.1 MPa$\sqrt{\text{mm}}$ and an intercept of 675 MPa. This slope is little changed from the value for the average microhardness of Cu (Fig. 5).

The Pd and Cu microhardness data presented here clearly indicate a large increase in hardness for the nanocrystalline samples compared to the annealed coarse-grained samples. Yet it is difficult to assess the magnitude of the strengthening effects of small grain size independent of weakening effects due to bulk sample defects. Maximum hardness data, too, are likely to be affected by near surface flaws. Any flaw (pore) intercepted by the indenter will result in a decrease in hardness below the hardness due to grain interactions. It is also clear that uncertainties in the precise grain size, and the presence of grain size distributions, can have a large effect on a plot of H_v vs $d^{-1/2}$ plot for nanometer grain size materials.

As described in Ref. 8, annealing of nanocrystalline Pd samples for 100 min made only a small change in their microhardness for annealing temperatures up to 700 °C (0.53 T_m). Beyond this point, H_v drops rapidly with increasing temperature. The decrease in hardness above 0.5 T_m suggests grain growth has occurred. Grain growth above 0.5 T_m has also been observed for nanocrystalline TiO_2[7] and Fe.[48] For a Pd

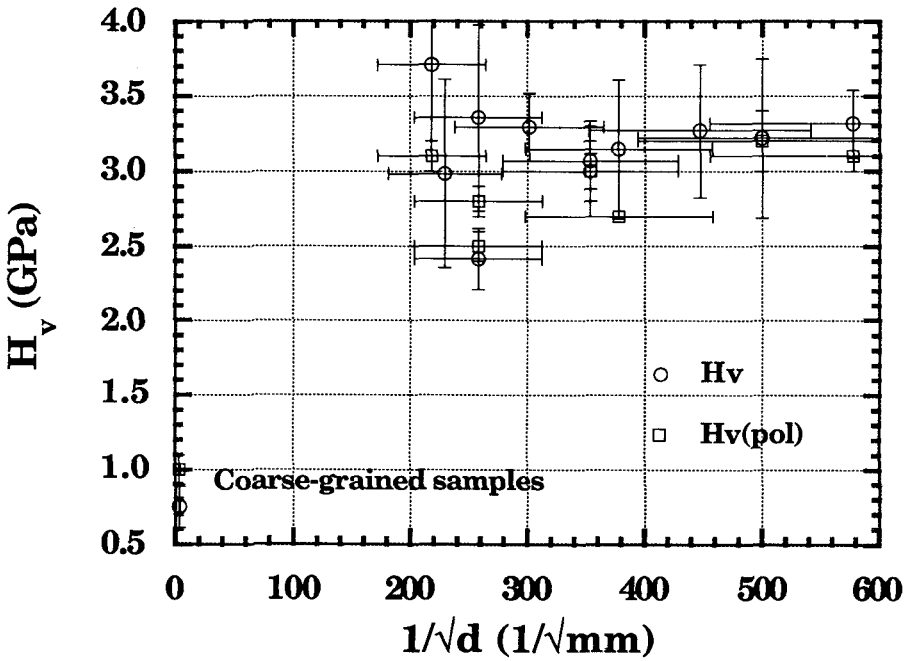

FIG. 4. Vickers microhardness of as-consolidated and well-polished nanocrystalline and coarse-grained Pd plotted as a function of $d^{-1/2}$.

https://doi.org/10.1557/JMR.1991.1012 Published online by Cambridge University Press

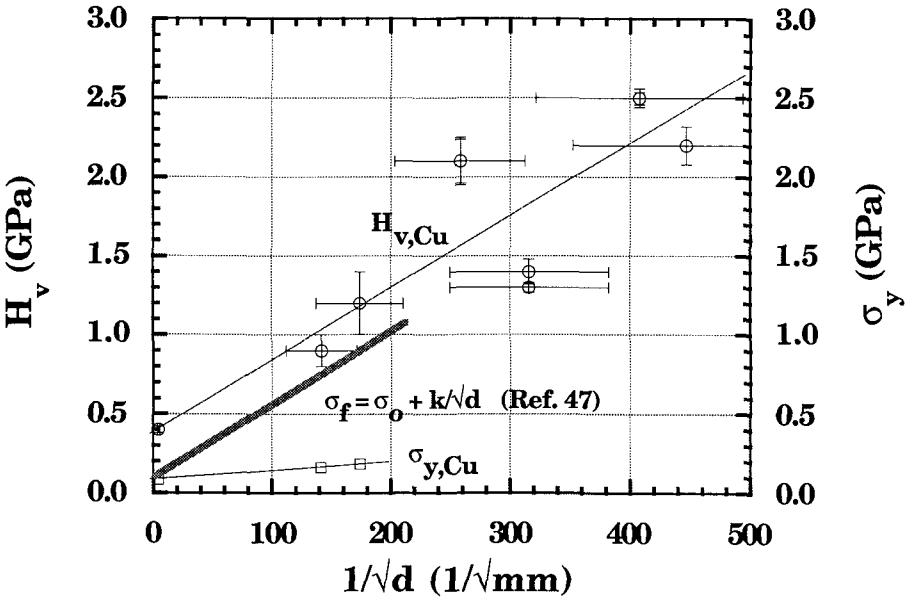

FIG. 5. Vickers microhardness of as-consolidated nanocrystalline and coarse-grained Cu and 0.2% offset yield stress of two nanocrystalline Cu samples and a coarse-grained sample, plotted as a function of $d^{-1/2}$. Also shown is a line that indicates the increase in flow stress in Cu; data from Ref. 47.

sample annealed in vacuum at 500 °C for 100 min, the mean grain size increased from 8 to 19 nm with no change in microhardness.[8]

B. Experimental details of tensile and creep tests

A miniaturized apparatus was designed and built (Fig. 7) to perform uniaxial tensile and creep tests on the small diameter samples (Fig. 8) described above. The load is applied by a magnetic actuator used in the dc mode, capable of supplying nominally 110 N force without air cooling or 220 N force with cooling. The machine is connected by an analog-digital signal conditioner/controller to a personal computer, and to an external load cell signal conditioner and an external LVDT transducer amplifier. A load cell with 445 N capacity is used to monitor applied loads. The load cell is connected to the actuator by a water-cooled brass adapter that prevents heat generated by the actuator from reaching the load cell. The upper stainless steel pull rod is connected directly to the load cell by a threaded mount. A lower pull rod is held in place by Woods metal. This arrangement allows alignment of the pull rod–sample assembly by gravity when the Woods metal is heated. An LVDT is used to monitor gage section elongation. Displacement sensitivity of the LVDT is better than 5×10^{-4} mm, and displacement

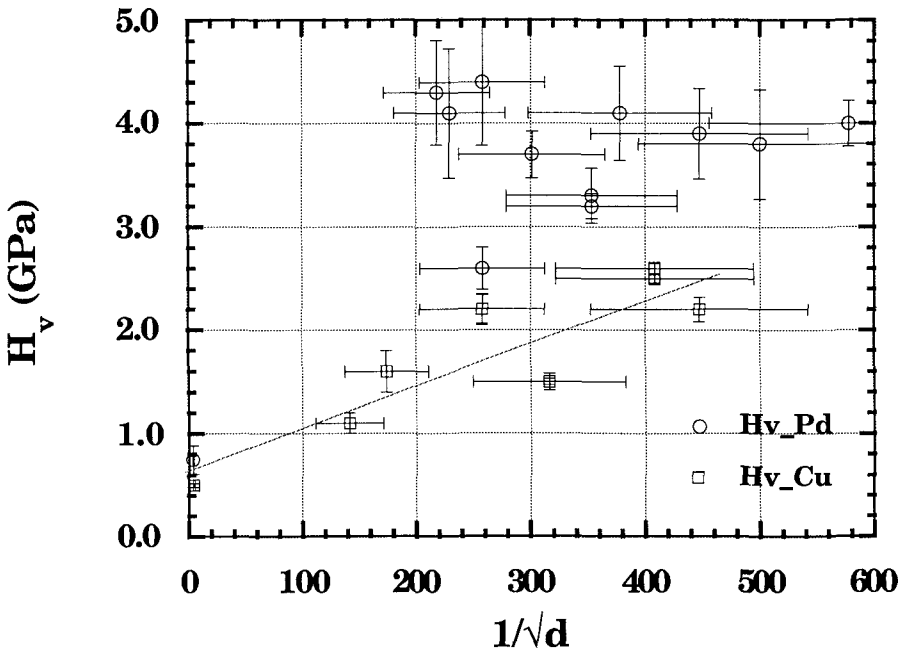

FIG. 6. Maximum Vickers microhardness of nanocrystalline and coarse-grained Pd and Cu samples as a function of $d^{-1/2}$.

https://doi.org/10.1557/JMR.1991.1012 Published online by Cambridge University Press

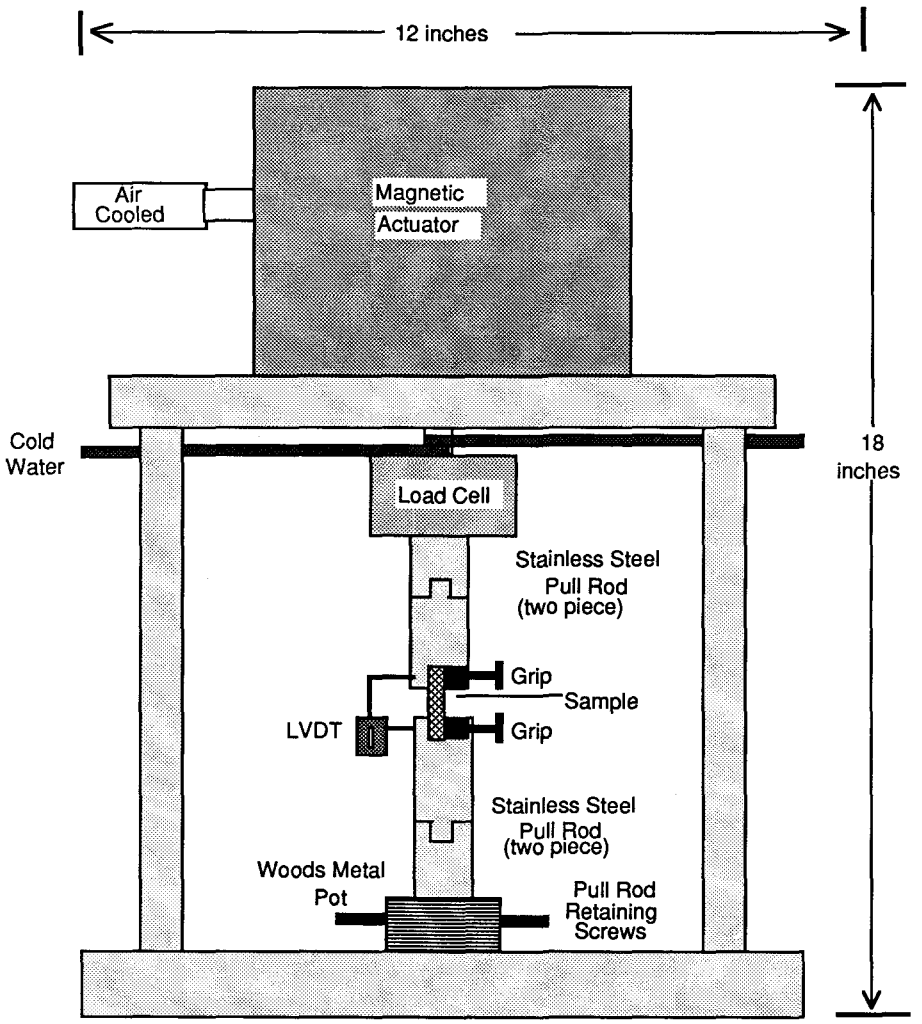

FIG. 7. Schematic diagram of the Baker–Nieman-1 (BN-1) tensile and creep test device used in this work.

capacity is about 0.13 mm. The LVDT could not be mounted directly on the sample due to the small sample size. It is connected to the pull rods at a point about 1 mm from the sample end of the grip in order to minimize elastic effects from the pull rods. The personal computer provides all digital-analog, voltage-load, and voltage-displacement conversions in addition to menu-driven test mode selection and data collection and storage routines.

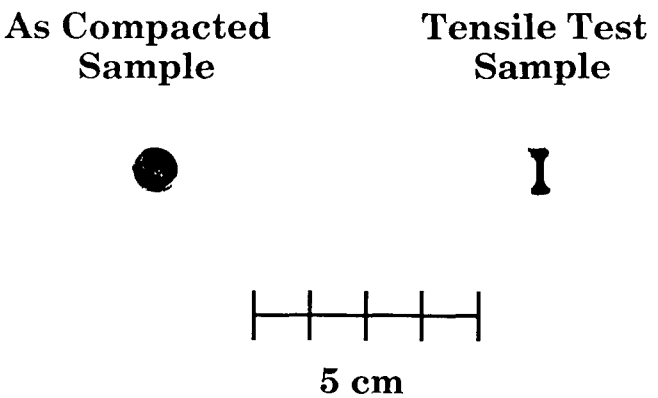

FIG. 8. Photomicrograph showing the dimensions of an as-consolidated sample (left) and a mechanical test sample (right) used in the tensile and creep tests.

Dogbone-shaped specimens (Fig. 8) for the tensile and creep tests were prepared from the as-compacted disks by electronic discharge machining. Sample gage lengths ranged from 3.5 mm to 2.0 mm, and sample gage widths were 1.4–2.0 mm. Samples thinner than about 180 μm could not be polished to remove surface flaws without breaking. The broad, flat surfaces of thicker samples were polished with 5 μm silicon carbide paper or 0.25 μm diamond paste, and a dental drill mounted on a dremmel tool was used to polish the thin edges of the sample.

C. Tensile test results

Tensile tests were performed on seven Pd and Cu nanocrystalline specimens to test their bulk mechanical properties. Samples of coarse-grained Pd and Cu were tested for comparison, but because the grain size of

https://doi.org/10.1557/JMR.1991.1012 Published online by Cambridge University Press

TABLE III. Tabulation of data from tensile tests on nanocrystalline Pd and Cu: E = Young's modulus, σ_y = yield stress, true ϵ = % true strain at failure, $\dot{\epsilon}$ = strain rate, (d) = displacement control, (l) = load control.

Sample	Grain size (nm)	E (GPa)	σ_y (MPa)	True ϵ (%)	$\dot{\epsilon}$ (/s)
Pd7061(d)	11	46	140	0.56	7×10^{-5}
Pd8031(l)	14	21	249	1.75	2×10^{-5}
Pd1202(l)	15	66	>330	>0.52	2×10^{-5}
Pd1203(l)	8	47	>200	>0.26	1×10^{-5}
Pd1205(l)	5	43	192	0.59	1×10^{-5}
Cu1103(l)	50	36	162	>2.2	1×10^{-5}
Cu1104(l)	25	45	185	>6.3	1×10^{-5}

these samples is large relative to the thickness and width of the tensile specimen, individual grains with a particular Schmid factor may dominate the measured mechanical behavior. The 0.2% offset was used as the yield stress. Samples of coarse-grained Cu showed a yield stress as low as 45 MPa and as high as 120 MPa. Typical values were around 85 MPa. The yield stress of coarse-grained Pd varied from 52 MPa to 85 MPa. Test results on two nanocrystalline samples of Pd have been reported previously.[9] Results of all tensile experiments on the nanocrystalline samples are tabulated in Table III.

The strength of the nanocrystalline samples is significantly improved by polishing to remove or reduce surface flaws. Figure 9 illustrates this improvement for Pd samples. One sample shows an apparent yield stress of 249 MPa and a total strain of $\leq$1.75% prior to failure. The apparent yield stress represents a fourfold increase over that of samples of coarse-grained Pd tested.[9] This sample was polished using 5 μm silicon carbide. A second sample, polished with 0.25 μm diamond paste, reached 330 MPa at the maximum load capacity of the test device without yielding or failing. The third sample, which was too thin to polish, failed at a low stress. The weakening effect of surface flaws on the strength of the samples is clear from this comparison.

The two samples of nanocrystalline Cu tested gave very interesting stress-strain curves. Significant plastic yielding was observed in both samples. The yield stress for the 50 nm sample [Fig. 10(a)] was measured as 162 MPa at a strain rate of 1.3×10^{-5}/s. A total engineering strain of 2.2% was produced before the load source capacity was reached and the test was terminated. Figure 10(b) compares the stress-strain curve for 25 nm nanocrystalline Cu and coarse-grained (50 μm) Cu. A yield stress of 185 MPa at a strain rate of 1.4×10^{-5}/s was observed for the 25 nm sample. This yield stress is over twice as large as that for the coarse-grained sample. Again, equipment limitations forced termination of the test at a total strain of 6.3% before failure of the nanocrystalline sample. The yield stress for commercially pure Cu ranges from 69–365 MPa,[49] with the highest values presumably representing highly cold worked material.

Low values of Young's modulus (E) were estimated for both nanocrystalline Cu samples from the initial slopes of the stress-strain curves. Lack of sensitivity in the strain measurements together with the usual problems with measuring E from stress-strain curves acted to limit the accuracy of the modulus measurements. Even so, it appears that Young's modulus of the

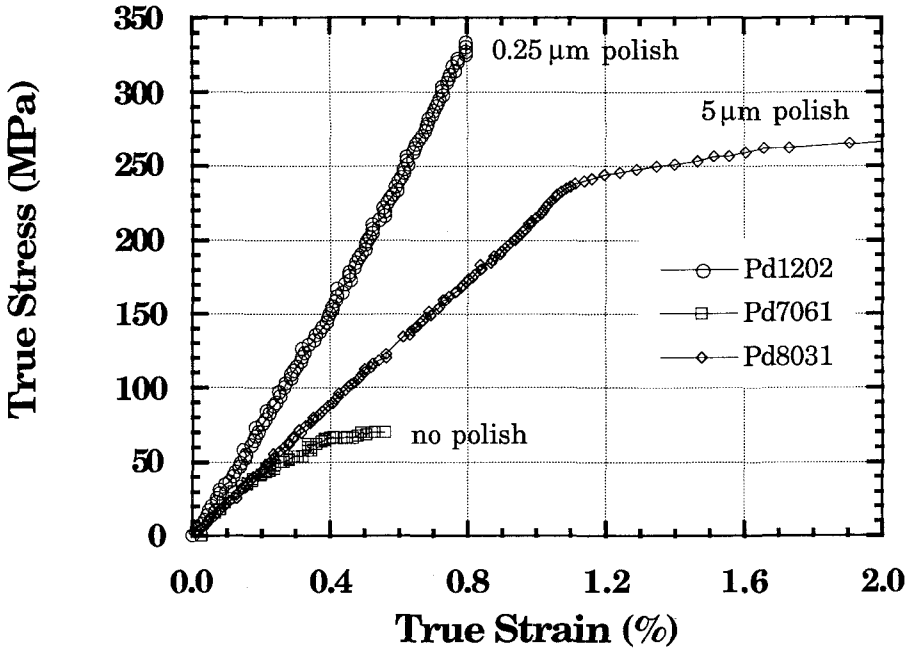

FIG. 9. Stress-strain results of tensile tests on nanocrystalline Pd, performed on BN-1, showing the beneficial effects of polishing to reduce the size of surface flaws.

https://doi.org/10.1557/JMR.1991.1012 Published online by Cambridge University Press

nanocrystalline Cu is significantly lower than that measured on conventional Cu (E = 130 GPa). Similar results were obtained in the case of Pd.[9] Possibly this is an effect of the porosity indicated by the density measurements. The true strain hardening exponent n, and strength coefficient K, given by $\sigma = K\epsilon^n$, are 0.12 and 308 MPa for the 50 nm nanocrystalline Cu sample, and 0.15 and 395 MPa for the 25 nm material. The true strain exponent for both Cu tests is well below the typical value of 0.3–0.35.[50]

The deformed nanocrystalline Cu samples were observed using optical and scanning electron microscopy to gain an insight into the deformation process. Optical microscopy clearly shows a surface texture resulting from tensile strain in the form of surface rumpling and linear bands (Fig. 11). This texture is conspicuous in the gage section. The strong bands of this localized surface deformation texture are oriented at about 60° to the tensile axis. Examination of the gage section by SEM showed little because of the low relief of this texture. However, one area in the gage section apparently showed a strong localized "shear band" oriented at an angle to the tensile axis of approximately 60°.

D. Creep test results

Equation (2) for Coble creep predicts a 10^9 enhancement in the creep rate of 10 nm grain size materials over that of a 10 μm grain size material. A 10^3 increase in grain boundary diffusivity in nanocrystalline Cu over the ordinary value, reported by Horváth *et al.*[21] and interpreted by others,[21–23] would further enhance the Coble creep rate. With this enhanced grain boundary diffusivity, Eq. (2) predicts a creep rate of $> 1 \times 10^{-5}$/s at 298 K and a stress of 100 MPa for 25 nm grain size Cu. The equipment used in the present experiments can measure creep rates down to about 10^{-9}/s.

Creep tests were carried out on nanocrystalline Pd and Cu to investigate this possibility of room temperature diffusional creep in these materials. Two nanocrystalline Cu samples and one of Pd were tested. The creep rate was also measured in coarse-grained Pd (100 μm) and Cu (50 μm). (The nanocrystalline Pd creep test results have been previously reported in Ref. 9.) The results of all creep tests on the nanocrystalline Cu and Pd samples are tabulated in Table IV.

Two creep tests were performed on the 25 nm grain size Cu sample. After an initial test at room temperature for 4.1 h under a stress of 145 MPa, the sample was unloaded and retested at 150 MPa for 14.2 h (Fig. 12). The initial creep rate of 1.2×10^{-6}/s dropped to 3.6×10^{-7}/s by about 4 h. By the end of the 150 MPa test, the creep rate had dropped to 1.4×10^{-7}/s. Clearly, the predicted diffusional creep rate was not observed. The shape of the creep curve is well described by the equation for logarithmic creep,[51] as can be seen from Fig. 12. The constant stress used in both tests is above 80% of the yield stress for this Cu sample and it is well above the 83 MPa stress at which the 50 μm Cu sample yielded.

A room temperature, constant load creep test on the 50 nm Cu sample resulted in a plot similar to that shown in Fig. 12. A constant stress of 103 MPa was used for this 17.8 h test. The creep rate fell from the initial value of 4.2×10^{-8}/s to 1.6×10^{-8}/s, near the end of the test. The total creep strain in this experiment was only 0.31%, about 12 times the sensitivity of the LVDT.

Similar results were obtained for nanocrystalline Pd samples.[9] A 10 nm grain size Pd showed a creep rate of 1.4×10^{-8}/s after 17.9 h at a constant stress of 130 MPa. A second test on the same nanocrystalline Pd sample using a stress of 148 MPa gave a creep rate of 7.3×10^{-9}/s after 18.2 h.

Creep tests were run on samples of coarse-grained Pd and Cu for comparison with the nanocrystalline sample data. Figure 13 shows results of a creep test on 50 μm grain-size Cu. The creep rate after 24 h under a stress of 74 MPa was 5.8×10^{-8}/s. A second test on the sample with a stress of 33 MPa produced a creep rate of 4.1×10^{-9}/s after 13.4 h. After 2 h of creep under a constant stress of 41 MPa, the strain rate in a sample of 100 μm Pd was 4.6×10^{-7}/s. While the creep rates and stresses are not exactly comparable in the corresponding nanocrystalline and coarse-grained experiments, it does not appear that creep is enhanced in the ultrafine-grained material at room temperature.

V. DISCUSSION

This study has described experiments on pure Pd and Cu designed to determine the effects of nanocrystalline grain size on mechanical properties such as Vickers microhardness, uniaxial tensile strength, and room temperature creep strength. Nanocrystalline samples produced by inert gas condensation and powder compaction in vacuum were shown to have mean grain sizes in the 5 to 50 nm range and significantly large internal strains, based on XRD analysis of line broadening. As-consolidated densities for six Pd samples and eight Cu samples range from 97–72% of standard density. Density data, in addition to optical and scanning electron microscopy observations, indicate the presence of pores and other types of processing flaws. Their presence may have a significant effect on mechanical properties, as demonstrated in microhardness and tensile tests.

A substantial increase in yield strength is observed in the nanocrystalline Pd and Cu specimens over that of their coarse-grained, annealed counterparts. This rise in strength appears to be appreciably less than pre-

https://doi.org/10.1557/JMR.1991.1012 Published online by Cambridge University Press

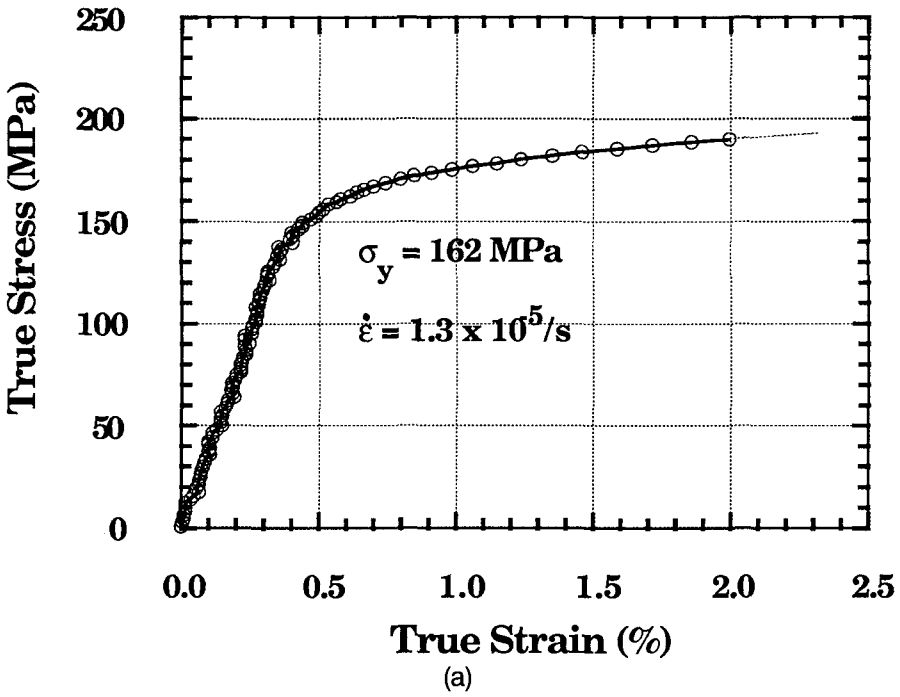

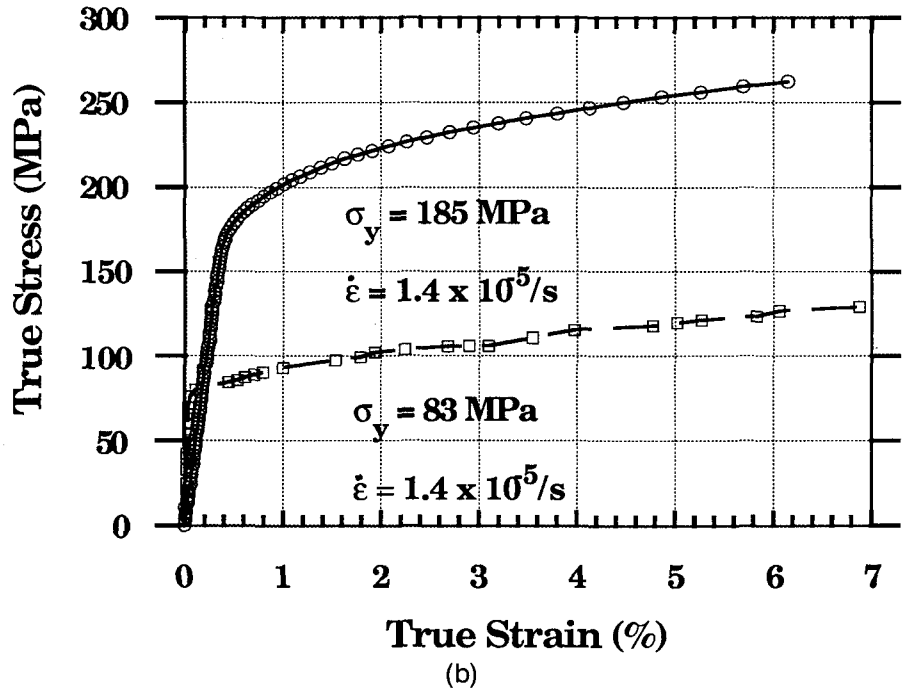

FIG. 10. (a) Stress-strain curve for nanocrystalline (50 nm) sample Cu1103, showing 0.2% offset yield stress. (b) Stress-strain curve for nanocrystalline (25 nm) sample Cu1104 and coarse-grained Cu sample (50 μm), showing 0.2% offset yield stresses.

dicted by extrapolation of Hall–Petch behavior from conventional to ultrafine grain size (Fig. 5). However, since yield strength of the strongest of the nanocrystalline Pd samples exceeded the capacity of the test machine, the actual strength, as well as the deviation from Hall–Petch behavior, remains uncertain. Removal of surface defects by polishing improves the measured strength of the samples (Fig. 9), as expected. This suggests that the "yield strengths" observed in Pd actually are determined by large (e.g., 0.1–1 μm) processing flaws and do not represent ultimate intrinsic material behavior. The large spatial variability in microhardness in Pd [Fig. 2(a)] is likely to be an artifact of these flaws. Similarly, lack of information on yield stress for Cu in the 5–15 nm grain size range limits any conclusions regarding the behavior of σ_y at these ultrafine grain sizes. Large ductility was observed in the two samples of nanocrystalline Cu before instrumental limitations

https://doi.org/10.1557/JMR.1991.1012 Published online by Cambridge University Press

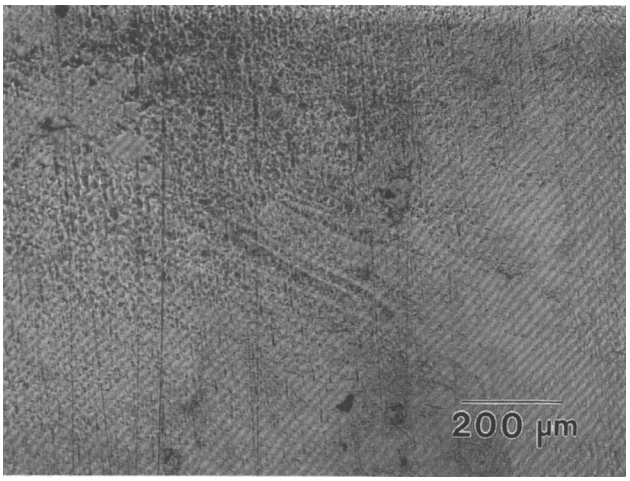

FIG. 11. Optical photomicrograph of nanocrystalline Cu tensile test specimen Cu1104 showing a strong localized "shear band" oriented at an angle to the tensile axis of approximately 60°.

truncated these tests. Deformation produced a strong surface texture in the specimen gage section, indicating strain localization occurred (Fig. 11).

The scatter in measured values of Vickers microhardness in the nanocrystalline Pd samples (plus some uncertainty in the grain size) prevents determination of the form of the dependence of H_v and σ_y on d at nanocrystalline grain sizes. However, there is no indication of a dramatic drop in strength at the smallest grain sizes, such as reported by Chokshi *et al.*[24] In fact, Cu samples show a strengthening with decreasing grain size in the 5–15 nm range. For comparable grain size material, we obtained significantly larger values of H_v for Pd and Cu than they reported.

Chokshi and co-workers attributed the significant downturn in strength that they reported over a small range of nanocrystalline grain size to the increasing importance of diffusional creep at the smallest grain sizes. Karch *et al.*[22] and Birringer *et al.*[23] also explained their observations on nanocrystalline ceramic materials as being due to diffusional creep. In the present investigation, direct measurements of nanocrystalline creep rates failed to detect room temperature diffusional creep. Creep was found to be some two orders of magnitude slower than predicted by Coble creep evaluated with the enhanced grain boundary diffusivity described in Refs. 21 and 23. The shape of the curves of creep strain versus time is described closely by the equation for logarithmic creep (Fig. 12). The lack of downturns in σ_y and microhardness at the smallest grain sizes; the absence of measurable room temperature diffusional creep; the similarity in XRD background levels for nanocrystalline and coarse-grained samples—all are consistent with the picture of grain boundaries in nanocrystalline metals that are similar in structure to those in conventional material, as shown in recent high resolution electron microscopy studies.[27,38]

TABLE IV. Tabulation of data from creep tests on nanocrystalline and coarse-grained Pd and Cu; ϵ = true strain (%), $\dot{\epsilon}$ = average strain rate.

Sample	Grain size (nm)	Time (min)	Constant stress (MPa)	$\dot{\epsilon}$ ($\times 10^{-8}$/s)	Apparent total ϵ (%)
Pd1203	8	1091	150	0.5	0.343
Pd1203	8	1071	130	1	0.409
PdStd	10^5	47	40	46	0.431
Cu1103	50	1070	100	4	0.545
Cu1104	25	45	145	7	1.203
Cu1104	25	850	150	14	1.161
CuStd	0.5×10^5	1440	74	6	0.052

The effect of analytical errors in making grain size estimates should be emphasized. Errors in grain size determination in the nanocrystalline size range can seriously distort a plot of experimental H_v (or σ_y) vs $d^{-1/2}$ data; predictions of low temperature diffusion creep rates, which have a d^{-3} dependence, also may be confounded.

The origin of the increased strength in the nanocrystalline material is not known, but restriction of dislocation activity (both generation and mobility) imposed by ultrafine grain size is believed to be the dominant factor. The length of potential Frank–Read sources is limited, both in grains and in grain boundaries. Also, even a modest number of dislocations in each grain would result in strengthening interactions. The strengthening effects of grain boundaries[52] are expected to be exceptionally important, since the relative volume of grain boundaries is large. Additionally, the large residual strains, observed by XRD and interpreted from HREM,[38,41] may also play a role in producing high strength. It has been observed that very large internal strains, driven by decrease in surface energy, are introduced when fine powders of metals are in contact.[42]

One might suppose that strength could be derived from cold work introduced during powder compaction. Dislocation densities on the order of $10^{15}/m^2$ have been reported for nanocrystalline Pd produced in the manner used for our samples.[38] However, for a 10 nm grain size, this amounts to only one dislocation per 10 grains, in contrast to normal cell structures produced during cold working. The nanocrystalline samples do not appear to be "cold-worked" in the conventional sense of a material strengthened by dislocation interactions.

The role of ultrafine pores or voids and impurity concentrations introduced during processing is also unknown. Small pores and trapped gases are known to strengthen coarse-grained metals at low temperatures,

https://doi.org/10.1557/JMR.1991.1012 Published online by Cambridge University Press

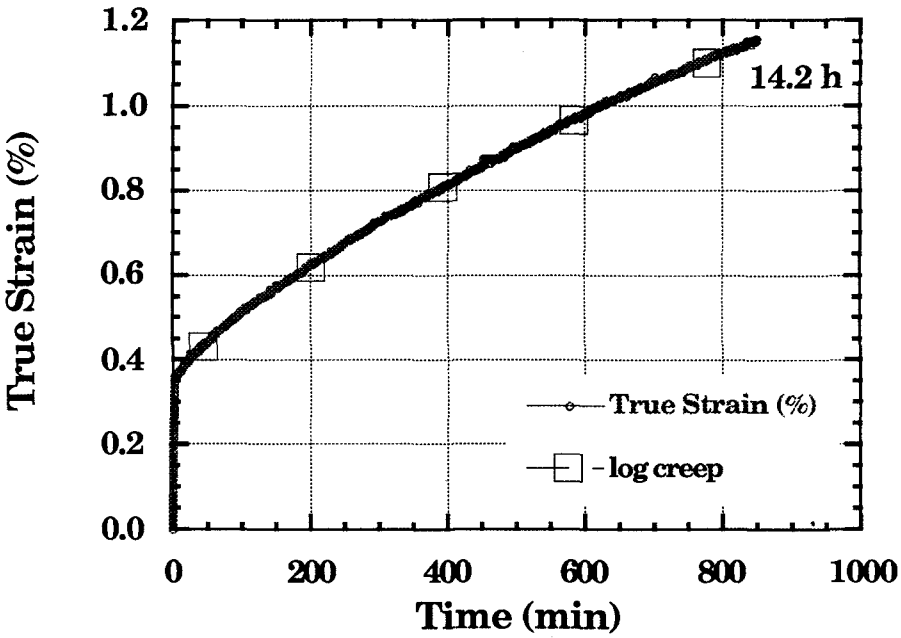

FIG. 12. Plot of true strain (%) versus time for a constant stress (150 MPa) room temperature creep test on a nanocrystalline (25 nm) Cu sample. Square symbols represent a fit to logarithmic creep dependence.

and impurities can pin grain boundaries. Large-scale pores, or other flaws, have been shown in the present work to limit the strength of the nanocrystalline samples. Some He could possibly be trapped in grains during inert gas condensation, or impurities adsorbed prior to consolidation. However, these effects are expected to be secondary to those cited above that result from decreasing grain size scale into the nanometer regime.

VI. CONCLUSIONS

(1) The yield strength and microhardness of nanocrystalline Pd and Cu specimens are substantially greater than those of annealed large-grained material. The increase in strength with decreasing grain size persists to the smallest-grained material studied.

(2) In many, if not all, of the nanocrystalline samples tested, strength is limited by processing flaws rather than by intrinsic behavior of the material.

(3) Detailed knowledge of the mechanisms that result in the increased strength of nanocrystalline material is lacking. Restrictions on dislocation activity (both generation and mobility) imposed by small grain size are assumed to be the dominant factor in raising strength. The large residual strains present in the sam-

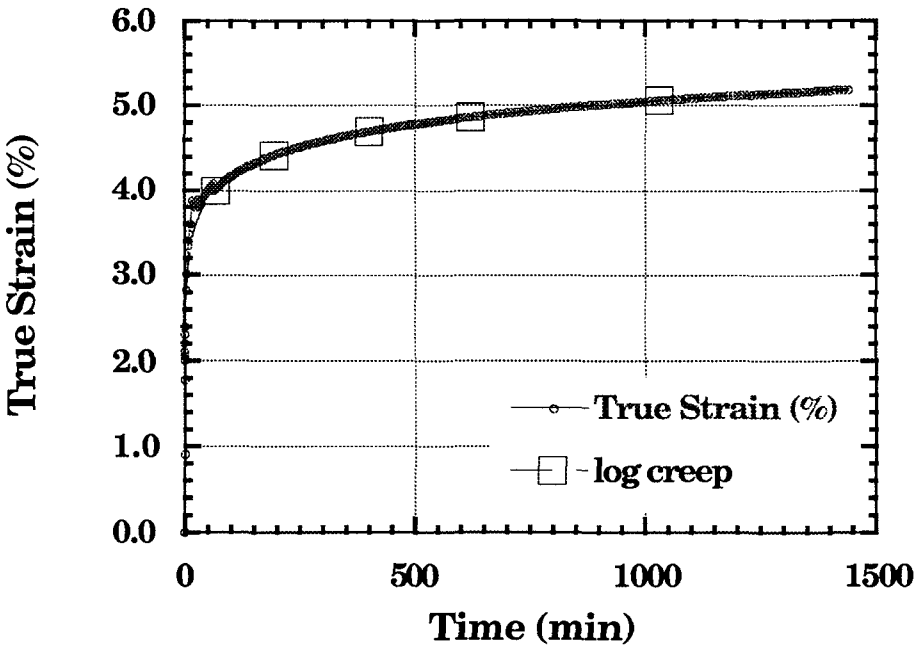

FIG. 13. Plot of true strain (%) versus time for a constant stress (74 MPa) room temperature creep test on a coarse-grained (50 μm) Cu sample. Square symbols represent a fit to logarithmic creep dependence.

https://doi.org/10.1557/JMR.1991.1012 Published online by Cambridge University Press

ples can also be expected to increase strength. Other factors, such as porosity or voids and impurity concentrations, may play a role as well.

(4) No room temperature diffusional creep was found in nanocrystalline Pd and Cu samples. Instead, samples appear to exhibit logarithmic creep typical of the behavior of conventional materials at room temperature.

ACKNOWLEDGMENTS

This research was supported by the National Science Foundation, Grant DMR-8320157, at Northwestern University and by the Department of Energy, Office of Basic Energy Sciences–Materials Sciences, Contract W-31-109-Eng-38, at Argonne National Laboratory.

REFERENCES

[1]H. Gleiter, in *Deformation of Polycrystals: Mechanisms and Microstructures,* edited by N. Hansen, A. Horsewell, T. Leffers, and H. Lilholt (Risø National Laboratory, Roskilde, 1981), p. 15.
[2]R. Birringer, U. Herr, and H. Gleiter, Suppl. Trans. Jpn. Inst. Metall. **27**, 43 (1986).
[3]R. Birringer, H. Gleiter, H-P. Klein, and P. Marquardt, Phys. Lett. **102A**, 365 (1984).
[4]C. G. Granqvist and R. A. Buhrman, J. Appl. Phys. **47**, 2200 (1976).
[5]R.W. Siegel and H. Hahn, in *Current Trends in the Physics of Materials,* edited by M. Yussouff (World Sci. Publ. Co., 1987), p. 403.
[6]H. Hahn, J. A. Eastman, and R.W. Siegel, Ceramic Trans. **1B**, 1115 (1988).
[7]R.W. Siegel, S. Ramasamy, H. Hahn, Li Zongquan, Lu Ting, and R. Gronsky, J. Mater. Res. **3**, 1367 (1988).
[8]G.W. Nieman, J. R. Weertman, and R.W. Siegel, Scripta Metall. **23**, 2013 (1989).
[9]G.W. Nieman, J. R. Weertman, and R.W. Siegel, Scripta Met. et Mater. **24**, 145 (1990).
[10]E. O. Hall, Proc. Phys. Soc. London **B64**, 747 (1951).
[11]N. J. Petch, J. Iron Steel Inst. **174**, 25 (1953).
[12]R.W. Armstrong, in *Yield, Flow and Fracture of Polycrystals,* edited by T. N. Baker (Applied Science Publishers, London, 1983), p. 1.
[13]N. Hansen, in *Yield, Flow and Fracture of Polycrystals,* edited by T. N. Baker (Applied Science Publishers, London, 1983), p. 311.
[14]A.W. Thompson, M. I. Baskes, and W. F. Flannagan, Acta Metall. **21**, 1017 (1973).
[15]R. L. Coble, J. Appl. Phys. **34**, 1679 (1963).
[16]A.W. Thompson, Acta Metall. **23**, 1337 (1977).
[17]U. Herr, J. Jing, R. Birringer, U. Gonser, and H. Gleiter, Appl. Phys. Lett. **50**, 472 (1987).
[18]X. Zhu, R. Birringer, U. Herr, and H. Gleiter, Phys. Rev. B **35**, 9085 (1987).
[19]H. E. Schaefer, R. Wurschum, M. Scheytt, R. Birringer, and H. Gleiter, Mater. Sci. Forum **15–18**, 955 (1987).
[20]J. Rupp and R. Birringer, Phys. Rev. B **36**, 7888 (1987).
[21]J. Horváth, R. Birringer, and H. Gleiter, Solid State Commun. **62**, 319 (1987).
[22]J. Karch, R. Birringer, and H. Gleiter, Nature **330**, 556 (1987).
[23]R. Birringer, H. Hahn, H. Höfler, J. Karch, and H. Gleiter, Defect and Diffusion Forum **59**, 17 (1988).
[24]A. H. Chokshi, A. Rosen, J. Karch, and H. Gleiter, Scripta Metall. **23**, 1679 (1989).
[25]C. A. Melendres, A. Narayanasamy, V. A. Maroni, and R.W. Siegel, J. Mater. Res. **4**, 1246 (1989).
[26]J. A. Eastman and L. J. Thompson, in *Interfaces between Polymers, Metals, and Ceramics,* edited by B. M. DeKoven, A. J. Gellman, and R. Rosenberg (Mater. Res. Soc. Symp. Proc. **153**, Pittsburgh, PA, 1989), p. 27.
[27]G. J. Thomas, R.W. Siegel, and J. A. Eastman, Scripta Met. et Mater. **24**, 201 (1990).
[28]J. E. Epperson, R.W. Siegel, J.W. White, T. E. Klippert, A. Narayanasamy, J. A. Eastman, and F. Trouw, in *Multicomponent Ultrafine Microstructures,* edited by L. E. McCandlish, B. H. Kear, D. E. Polk, and R.W. Siegel (Mater. Res. Soc. Symp. Proc. **132**, Pittsburgh, PA, 1989), p. 15.
[29]J. A. Eastman, Y. X. Liao, A. Narayanasamy, and R.W. Siegel, in *Processing Science of Advanced Ceramics,* edited by I. A. Aksay, G. L. McVay, and D. R. Ulrich (Mater. Res. Soc. Symp. Proc. **155**, Pittsburgh, PA, 1989), p. 255.
[30]*Handbook of Chemistry and Physics,* 62nd ed., edited by R. C. Weast (CRC Press, Boca Raton, FL, 1981), p. B2.
[31]R. M. German, *Powder Metallurgy Science* (Metal Powder Industries Federation, 1984), p. 113.
[32]H. F. Fischmeister, E. Artz, and L. R. Olsson, Powder Met. **4**, 179 (1978).
[33]E.Y. Gutmanas, A. Rabinkin, and M. Roitberg, Scripta Metall. **13**, 11 (1979).
[34]B. E. Warren, *X-ray Diffraction* (Addison-Wesley, Reading, MA, 1969), p. 251.
[35]L. H. Schwartz and J. B. Cohen, *Diffraction from Materials,* 2nd ed. (Springer-Verlag, Berlin, 1987), p. 372.
[36]A. Guinier, *X-ray Diffraction in Crystals, Imperfect Crystals and Amorphous Bodies* (W. H. Freeman and Co., San Francisco, CA, 1970), p. 121.
[37]R. K. Nandi, H. K. Kuo, W. Schlosberg, G. Wissler, J. B. Cohen, and B. Crist, J. Appl. Cryst. **17**, 22 (1984).
[38]W. Wunderlich, I. Ishida, and R. Maurer, Scripta Met. et Mater. **24**, 403 (1990).
[39]R. de Keijser, E. J. Mittemeijer, and H. C. F. Rozendaal, J. Appl. Cryst. **16**, 309 (1983).
[40]G.W. Nieman and J. R. Weertman, Proc. of the Morris E. Fine symp., Detroit (1990), edited by P. K. Liaw *et al.* (The Minerals, Metals and Materials Society, Warrendale, PA, 1991), p. 243.
[41]N. J. Long, R. F. Marzke, M. McKelvy, and W. S. Glaunsinger, Ultramicroscopy **20**, 15 (1986).
[42]K. E. Easterling and A. R. Thölén, Powder Met. **16**, 112 (1973).
[43]E. Hellstern, H. J. Fecht, Z. Fu, and W. L. Johnson, J. Appl. Phys. **65**, 305 (1989).
[44]D. Tabor, *The Hardness of Metals* (Oxford University Press, London, 1951).
[45]M. A. Meyers and K. K. Chawla, *Mechanical Metallurgy Principles and Applications* (Prentice-Hall Inc., Englewood Cliffs, NJ, 1964), p. 600.
[46]G. M. Pharr and W. C. Oliver, J. Mater. Res. **4**, 94 (1989).
[47]N. Hansen and B. Ralph, Acta Metall. **30**, 411 (1982).
[48]E. Hort, Diploma Thesis, Universität des Saarlandes, Saarbrücken (1986).
[49]*Metals Handbook Desk Edition,* edited by H. B. Boyer and T. L. Gall, 7-2 (1985).
[50]R.W. Hertzberg, *Deformation and Fracture Mechanics of Engineering Materials,* 2nd ed. (John Wiley and Sons, New York, 1983), p. 17.
[51]J. Weertman and J. R. Weertman, in *Physical Metallurgy, Part II,* 3rd ed., edited by R.W. Cahn and P. Haasen (North Holland, Amsterdam, 1983), p. 1259.
[52]J. P. Hirth, Metall. Trans. **3**, 3047 (1972).

https://doi.org/10.1557/JMR.1991.1012 Published online by Cambridge University Press